

Nonbonding Orbitals in Fullerenes: Nuts and Cores in Singular Polyhedral Graphs

Irene Sciriha

Department of Mathematics, Faculty of Science, University of Malta, Msida, Malta

Patrick W. Fowler*

Department of Chemistry, University of Sheffield, Sheffield S3 7HF, U.K.

Received March 16, 2007

A zero eigenvalue in the spectrum of the adjacency matrix of the graph representing an unsaturated carbon framework indicates the presence of a nonbonding π orbital (NBO). A graph with at least one zero in the spectrum is *singular*; nonzero entries in the corresponding zero-eigenvalue eigenvector(s) (*kernel* eigenvectors) identify the *core* vertices. A *nut* graph has a single zero in its adjacency spectrum with a corresponding eigenvector for which all vertices lie in the core. *Balanced* and *uniform* trivalent (cubic) nut graphs are defined in terms of $(-2, +1, +1)$ patterns of eigenvector entries around all vertices. In balanced nut graphs all vertices have such a pattern up to a scale factor; uniform nut graphs are balanced with scale factor one for every vertex. Nut graphs are rare among small fullerenes (41 of the 10 190 782 fullerene isomers on up to 120 vertices) but common among the small trivalent polyhedra (62 043 of the 398 383 nonbipartite polyhedra on up to 24 vertices). Two constructions are described, one that is conjectured to yield an infinite series of uniform nut fullerenes, and another that is conjectured to yield an infinite series of cubic polyhedral nut graphs. All hypothetical nut fullerenes found so far have some pentagon adjacencies: it is proved that all uniform nut fullerenes must have such adjacencies and that the NBO is totally symmetric in all balanced nut fullerenes. A single electron placed in the NBO of a uniform nut fullerene gives a spin density distribution with the smallest possible (4:1) ratio between most and least populated sites for an NBO. It is observed that, in all nut-fullerene graphs found so far, occupation of the NBO would require the fullerene to carry at least 3 negative charges, whereas in most carbon cages based on small nut cubic polyhedra, the NBO would be the highest occupied molecular orbital (HOMO) for the uncharged system.

1. INTRODUCTION

Graph theory gives tools for the classification of the structures and electronic properties of the all-carbon fullerene molecules, C_n . In particular, diagonalization of the adjacency matrix yields π orbital energies (eigenvalues) and π molecular orbitals (eigenvectors) within the Hückel approximations, from which chemically useful conclusions may often be drawn. For example, Hückel theory predicts the characteristic electron deficiency of the typical fullerene¹ and gives systematic rules for the occurrence among the fullerenes of properly closed-shell π configurations (those with bonding highest occupied molecular orbital (HOMO) and antibonding or nonbonding lowest unoccupied molecular orbital (LUMO)).² Closed shells of this type are rare among the smaller fullerenes: for $n < 112$ the known closed shells are confined to 35 leapfrog and 3 cylindrical isomers² (out of 4 032 334 fullerenes, of which 8093 have disjoint pentagons³). For $n \geq 112$, a third sparse class, the so-called *sporadic* closed shells, also appears.²

Also comparatively rare are fullerenes with one or more exactly nonbonding π orbitals (NBO), i.e., with one or more zero eigenvalues of the adjacency matrix \mathbf{A} . A fullerene, or any graph, with at least one zero eigenvalue is said to be *singular*. Nonbonding orbitals in generally electron-deficient molecules such as fullerenes are of direct chemical interest

as they represent cases where the molecule (with some particular total charge) would be predicted to tolerate both removal and addition of electrons, and the form of the NBO then gives information about the spin distribution in the derived radicals. From this point of view, the NBO is of most interest when it is either the HOMO or the LUMO of a fullerene with small or zero total charge. In the chemical context,⁴ the presence of NBOs in some fullerenes and related polyhedra has been rationalized by relating the orbital patterns to the four basic nonbonding combinations on the graphite sheet, in a pictorial version of the ‘zone-folding’ argument used for nanotubes and polyhex tori.⁵

In a mathematical context, an equivalent question has been posed about arbitrary graphs:^{6,7} Which particular structural features does a singular graph possess? Graphs with exactly one zero eigenvalue of \mathbf{A} were considered first,⁶ as for this case there is no masking of the effect of one eigenvector by another in the same eigenspace. Graphs of this kind for which the eigenvector corresponding to the zero eigenvalue (the *kernel* vector) has no zero entries are *nut graphs*. For graphs with more than one zero eigenvalue, it was concluded that, in a basis where the total number of nonzero entries of the basis vectors is a minimum, the vectors determine specific subgraphs (*minimal configurations*). This earlier work on arbitrary graphs prompted the present study of the nullity properties of some polyhedral chemical graphs, in which the questions addressed are as follows: (1) Can fullerenes and

* Corresponding author e-mail: P.W.Fowler@sheffield.ac.uk.

Table 1. Singular Fullerenes C_n for $n \leq 120$ with Pentagon Adjacencies, Listed by Nullity η and Labeled by Their Place in Full Spiral Lexicographic Order^a

20:1(9,c)		$\eta = 4$		
		$\eta = 2$		
24:1(13,c)	36:5(19,c)	36:13(19)	36:15(19,c)	38:2(20)
42:45(22)	44:72(23)	44:80(23)	48:189(25,c)	56:3(29)
60:1374(31,c)	60:1784(31,c)	68:2189(35)	72:6414(37,c)	72:8049(37)
72:11182(37,c)	74:2(38)	84:22660(43,c)	86:20964(44)	92:3(47)
96:65052(49,c)	108:161702(55,c)	110:3(56)	120:362261(61,c)	
		$\eta = 1$		
28:1(15,16)	32:5(18,12*)	36:9(20,20)	38:12(20,24)	40:38(22,24)
40:39(22,20)	44:13(24,16*)	44:24(24,24)	44:55(23,32)	44:61(23,38)
44:75(23,24)	44:83(24,32)	48:160(25,44)	48:175(26,44)	48:186(26,24)
50:43(27,28)	50:157(27,18*)	52:376(28,46)	52:431(28,32)	52:432(28,32)
52:435(28,32)	56:35(30,20*)	56:393(30,20*)	58:1137(30,30)	60:221(32,36)
60:1247(32,52)	60:1782(32,48)	60:1805(32,40)	60:1810(31,40)	62:629(33,22*)
62:1799(32,44)	64:70(34,58)	64:1268(34,48)	64:1801(33,58)	64:3331(34,60)
68:78(36,24*)	68:405(36,40)	68:409(36,40)	68:1158(36,24*)	68:1980(36,64)
68:6015(36,48)	68:6140(36,36)	68:6331(36,24*)	74:1979(39,26*)	74:2962(39,26*)
76:8871(39,64)	76:8879(40,64)	76:12651(40,48)	76:19143(40,52)	78:23791(40,48)
80:168(42,28*)	80:3246(42,28*)	80:5306(42,28*)	80:31908(41,78)	82:37768(43,48)
84:1064(44,52)	84:7375(44,52)	84:18295(43,68)	86:4586(45,30*)	86:18225(45,60)
86:46893(45,60)	84:51545(44,64)	86:47231(45,60)	86:63338(45,48)	86:63512(45,30*)
88:25976(46,60)	88:81605(46,72)	90:536(47,72)	90:82841(47,82)	92:304(48,32*)
92:1623(48,56)	92:7044(48,32*)	92:13153(48,32*)	92:13188(48,32*)	92:13426(48,32*)
92:59039(48,62)	92:125179(48,72)	92:126025(48,32*)	92:126154(48,62)	92:126311(48,32*)
96:170895(50,94)	96:171222(50,90)	96:187896(50,72)	98:9622(51,34*)	98:18465(51,34*)
98:19394(51,34*)	98:221835(51,76)	98:226396(51,34*)	100:112387(52,64)	100:112388(52,64)
100:282237(52,80)	104:559(54,36*)	104:14414(54,36*)	104:30233(54,36*)	104:398924(54,36*)
104:401317(54,36*)	104:401325(54,36*)	106:9071(55,80)	106:467835(55,60)	108:3318(56,68)
108:592297(56,106)	110:19095(57,38*)	110:36041(57,38*)	110:36076(57,38*)	110:37610(57,38*)
110:38292(57,38*)	110:155290(57,78)	110:625591(57,76)	110:625628(57,76)	110:681160(57,76)
110:691942(57,38*)	112:815346(58,96)	112:840551(58,84)	112:856010(58,92)	116:923(60,40*)
116:4675(60,72)	116:4679(60,72)	116:27417(60,40*)	116:50288(60,40*)	116:52313(60,40*)
116:53462(60,40*)	116:54322(60,40*)	116:56855(60,40*)	116:60468(60,40*)	116:704703(59,112)
116:1143730(60,40*)	116:1195823(60,72)			

^a Nut fullerenes also have $\eta = 1$ but are listed separately (Table 3). For $\eta > 1$, the number in parentheses is p_+ , the number of strictly positive eigenvalues in the adjacency spectrum, and a symbol c indicates that the fullerene is a core; for $\eta = 1$, the first number is p_+ , and the second is the number of nonzero entries in the null eigenvector, marked by a star in cases where the core is an independent set.

other chemically relevant trivalent polyhedra be nut graphs?
(2) Given that they can, how common are these nut graphs, and how can they be constructed?

Some of the mathematical aspects of these questions have been considered elsewhere.^{8,9} Here we consider the chemical description and implications of these questions about nullity in fullerenes and related objects.

To answer these questions, graphs for general C_n -fullerenes ($n \leq 120$), isolated-pentagon (IP) C_n -fullerenes ($n \leq 150$), and trivalent polyhedra ($n \leq 24$) were generated using the spiral algorithm² for the fullerenes and the plantri program¹⁰ for small trivalent polyhedra. Adjacency spectra were obtained by numerical diagonalization of the adjacency matrix for each graph, and where singular graphs were found, the eigenvector(s) with zero eigenvalue were analyzed for various patterns in the signs and magnitudes of their entries. Material obtained from these computer searches is collected in Tables 1–4 toward the middle and end of the paper, but specific examples are sometimes quoted in advance or shown in earlier figures, in order to help with the introduction of the various concepts.

The structure of the paper is as follows. First, section 2 recalls definitions and notation, makes the connection between molecules and graphs, and defines the substructures (minimal configuration, core, periphery) that go to make up a singular graph. In section 3, we investigate singular

Table 2. Isolated-Pentagon Singular Fullerenes C_n for $n \leq 150$ Listed by Nullity η and Labeled by Their Place in Isolated-Pentagon Spiral Lexicographic Order^a

84:24(42)			$\eta = 3$		
			$\eta = 1$		
70:1(35,40)	84:16(43,64)	94:134(48,54)			
100:1(50,60)	100:438(52,96)	104:822(54,60)			
104:823(54,60)	110:518(56,72)	120:10606(60,72)			
130:1(65,80)	130:37423(66,78)	136:18743(69,96)			
140:75226(72,84)	144:71038(74,96)	148:268934(76,120)			

^a No nut fullerenes are found within this set. For $\eta > 1$, the number in parentheses is p_+ , the number of strictly positive eigenvalues in the adjacency spectrum; for $\eta = 1$, the first number is p_+ , and the second is the number of nonzero entries in the null eigenvector.

fullerenes and show that some of them are indeed nut graphs. We give some statistics and observations on singular and nut graphs among the C_n -fullerenes for $n \leq 120$, fullerenes with isolated pentagons for $n \leq 150$ (in section 3), and the cubic polyhedral graphs for $n \leq 24$ (section 4). For example, by inspecting the kernel eigenvector entries, we identify three classes of nut graphs. For two of them we find regularities in vertex count. For one class we find a method of constructing infinite series of conjectural fullerene nut graphs. In the section on nut graphs based on the more general singular cubic polyhedra (section 4), another construction is

Table 3. Nut Fullerenes C_n for $n \leq 120^a$

isomer $n:m$	\mathcal{G}												p_+	Γ	uniform?	N_p	
36:14	D_{2d}	1	2	4	7	9	10	12	13	14	16	18	20	20	a_1	U(2)	12
42:12†	C_s	1	2	3	4	7	11	16	18	19	20	21	22	22	a'	N(10)	12
44:14	C_2	1	2	3	4	7	11	14	18	21	22	23	24	24	a	N(14)	14
48:16	D_2	1	2	3	4	7	10	18	21	23	24	25	26	26	a	U(2)	14
48:169	D_2	1	2	4	7	9	13	17	19	21	23	25	26	26	a	B(3)	8
52:313	D_{2d}	1	2	3	10	14	15	18	19	21	23	27	28	28	b_2	N(8)	12
52:335	C_2	1	2	4	7	9	13	19	20	23	24	25	27	28	b	N(32)	7
60:43	D_2	1	2	3	4	7	10	23	26	29	30	31	32	32	a	U(2)	14
60:1169	C_2	1	2	4	7	9	19	22	23	26	28	29	32	32	a	N(15)	7
60:1196	D_2	1	2	4	7	10	14	20	24	27	30	31	32	32	a	U(2)	10
60:1197	D_2	1	2	4	7	10	14	25	26	28	29	30	32	32	a	U(2)	10
60:1279†	C_2	1	2	4	7	12	16	18	22	25	28	31	32	31	a	N(5)	6
60:1621	D_2	1	2	4	12	13	14	18	25	26	28	30	32	32	a	U(2)	8
72:97	D_2	1	2	3	4	7	10	29	32	35	36	37	38	38	a	U(2)	14
72:9897	D_2	1	2	4	15	18	22	23	26	29	30	32	35	38	a	U(2)	8
82:25969	C_2	1	2	4	12	19	26	28	31	34	35	36	39	43	a	N(72)	4
84:197	D_2	1	2	3	4	7	10	36	39	41	42	43	44	44	a	U(2)	14
84:19272	D_2	1	2	4	7	10	14	33	36	37	40	42	44	44	a	U(2)	10
84:22788	D_2	1	2	4	8	11	12	31	39	40	42	43	44	44	a	U(2)	10
84:28619	D_{2h}	1	2	4	12	13	14	34	35	36	40	43	44	44	a_g	U(2)	8
84:28620	D_{2h}	1	2	4	12	13	14	34	36	40	41	43	44	44	a_1	U(2)	8
84:38210	D_{2d}	1	2	4	15	21	26	32	33	37	39	40	41	44	a_1	U(2)	8
84:41799	D_2	1	2	4	18	22	23	28	29	33	36	37	44	44	a	U(2)	8
84:51548	D_{2h}	1	2	12	17	19	21	25	27	34	39	42	44	44	a_g	N(8)	2
96:367	D_2	1	2	3	4	7	10	41	44	47	48	49	50	50	a	U(2)	14
96:114148	D_2	1	2	4	15	26	31	38	43	44	46	47	48	50	a	U(2)	8
96:134237	D_2	1	2	4	22	23	28	34	39	40	43	49	50	50	a	U(2)	8
96:137750	D_{2d}	1	2	4	28	32	36	37	38	41	42	46	47	50	a_1	U(2)	8
96:139895	D_2	1	2	7	23	24	25	30	31	32	44	48	50	50	a	U(2)	8
108:634	D_2	1	2	3	4	7	10	47	50	53	54	55	56	56	a	U(2)	14
108:140651	D_2	1	2	4	7	10	14	44	48	51	54	55	56	56	a	U(2)	10
108:140652	D_2	1	2	4	7	10	14	49	50	52	53	54	56	56	a	U(2)	10
108:202011	D_2	1	2	4	12	13	14	43	49	50	52	54	56	56	a	U(2)	8
108:277775	D_2	1	2	4	15	26	34	38	42	46	52	53	55	56	a	U(2)	8
108:337625	D_2	1	2	4	18	28	29	34	45	48	49	50	54	56	a	U(2)	8
108:345562	D_2	1	2	4	22	23	34	39	42	43	44	50	51	56	a	U(2)	8
120:1069	D_2	1	2	3	4	7	10	54	57	59	60	61	62	62	a	U(2)	14
120:603082	D_2	1	2	4	15	26	38	45	52	56	57	61	62	62	a	U(2)	8
120:756134	D_2	1	2	4	18	28	29	46	47	48	59	60	61	62	a	U(2)	8
120:779562	D_2	1	2	4	22	23	34	42	50	53	54	60	62	62	a	U(2)	8
120:1653993	D_{2d}	1	2	19	22	26	29	35	38	42	45	59	62	62	a_1	N(5)	4

^a Isomers are labeled by position in full spiral lexicographic order, point group (\mathcal{G}), pentagon positions in the face spiral, number of strictly positive eigenvalues (p_+), irreducible representation of the unique zero eigenvector (Γ), characterization as uniform (U), balanced (B), or neither (N), with numbers of distinct eigenvector entries, and number of pentagon adjacencies (N_p). Zero is eigenvalue $n/2 + 2$ in the two cases marked †, otherwise $n/2 + 3$.

Table 4. Statistics for Singular Trivalent Polyhedra with $n \leq 24$ Vertices

n	polyhedra	bipartite	$\eta \neq 0$	$\eta = 1$					
				all	nuts = U + B + N	2	3	4	5
4	1	0	0	0		0	0	0	0
6	1	0	1	0		0	1(0)	0	0
8	2	1	0	0		0	0	0	0
10	5	0	1	1		0	0	0	0
12	14	1	11	2		2 = 2 + 0 + 0	7(0)	0	2(1)
14	50	1	8	7		0	1(0)	0	0
16	233	2	70	67		0	1(0)	2	0
18	1249	2	613	322		285 = 235 + 38 + 12	280(1)	1	10(0)
20	7595	8	1225	1123		0	99(1)	2	1
22	49 566	8	11 330	10 548		0	623(3)	158	1(0)
24	339 722	32	120 628	81 127		62 043 = 35 632 + 14 022 + 12 389	37 567(10)	945	987(20)

given for an open-ended series of non-fullerene nut or core graphs. We end (section 5) by commenting on the relevance of these results to the chemistry of fullerenes. In the appropriate charge state, a nut-graph fullerene with a half-occupied NBO would be predicted to have nonzero spin density at all sites and so would have markedly different reactivity from the more usual types of radical, where the spin density at some sites vanishes.

2. DEFINITIONS

2.1. Graphs. A graph $G(\mathcal{V}, \mathcal{E})$ having a vertex set $\mathcal{V}(G) = \{v_1, v_2, \dots, v_n\}$ and a set \mathcal{E} of $m(G)$ edges joining distinct pairs of vertices is said to be of order $n(G)$ ($= n$) and size $m(G)$ ($= m$). The valency of a vertex v is the number of edges incident to v . A ρ -regular graph is one for which the valency is ρ for each vertex; a 3-regular graph is known as

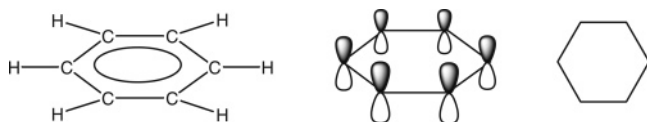


Figure 1. Stages in the idealization of an unsaturated molecule as a graph (left to right) from a molecular structure as illustrated for benzene, to π system, to graph.

cubic in mathematics and *trivalent* in chemistry. A subset of \mathcal{V} is said to be *independent* in G if there are no edges joining pairs of distinct vertices; the *independence number* $\alpha(G)$ is the maximum order of such a subset. A subset of \mathcal{V} , taken together with those edges in ϵ that join members of this subset, defines an *induced subgraph* of G . The *complete graph* K_n has n vertices and an edge between every pair of distinct vertices. The *cycle* C_n has n vertices, is connected, and the valency of each vertex is two. The graph $G(X, Y, \epsilon)$ is *bipartite* if there is a partition of its vertex set into disjoint sets X and Y such that each edge in ϵ joins a vertex of X to a vertex of Y .

2.2. Chemical Graphs. In a molecular graph of an all-carbon or hydrocarbon system, vertices stand for unsaturated C atoms and so have valency at most three, and edges stand for the underlying carbon–carbon σ bonds (Figure 1).

A *fullerene* is an all-carbon molecule which, like polycyclic aromatic hydrocarbons and graphite, is built of sp^2 -hybridized atoms, linked by σ bonds, each carbon center donating one electron and one atomic p orbital to an unsaturated π system. The molecular graph of a fullerene is cubic and has a planar embedding. In 3D it can be realized as a pseudospherical polyhedral framework, its faces consisting of pentagons and hexagons only, each C atom forming σ bonds to three nearest neighbors. From the Euler relation for spherical polyhedra, it follows that a fullerene has exactly 12 pentagonal faces and has an even number of C atoms, $n = 20 + 2h$, where h is the number of hexagonal faces, $h = 0$ or $h > 1$.¹¹ Fullerenes are denoted by their chemical formula C_n , and, when it is necessary to distinguish between isomers, by their place in the order of generation by the spiral algorithm,² so that, e.g., $C_{32}:5$ is the fifth isomer in the set of six possible fullerenes on 32 vertices. (Depending on context, the ordering used may be the full spiral order of general fullerene isomers, or the order of isolated-pentagon fullerenes only, so that, e.g., the experimental isomer of C_{60} , in the isolated-pentagon series known as $C_{60}:1$, may also be referred to as $C_{60}:1812$ in the context of general fullerenes.)

The *adjacency matrix* $\mathbf{A}(G)$ (or simply \mathbf{A}) of a graph G is an $n \times n$ symmetric matrix $[a_{ij}]$ such that $a_{ij} = 1$ if i and j are connected by an edge and 0 otherwise. This describes G completely (up to isomorphism). A graph G is *singular* if $\mathbf{A}(G)$ has an eigenvalue zero. There exist $\eta(G)$ (or simply η) linearly independent nonzero vectors \mathbf{x} , called *kernel eigenvectors* in the nullspace ϵ_0 of \mathbf{A} , satisfying $\mathbf{A}\mathbf{x} = 0$. The multiplicity (in chemical language, the degeneracy) η of the zero eigenvalue of $\mathbf{A}(G)$ is the *nullity* of \mathbf{A} and corresponds to the number of NBO predicted in Hückel Theory for the π system of the molecule with molecular graph G . The *rank* of G , denoted by $r(G)$, is the rank of $\mathbf{A}(G)$, which is $n(G) - \eta(G)$.

Each eigenvector \mathbf{x} corresponds in Hückel Theory¹² to a π molecular orbital (MO) of the carbon framework, with the entry on vertex i giving the contribution of the local p

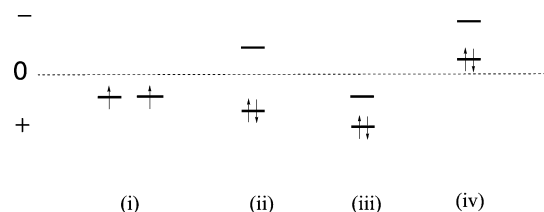


Figure 2. Illustrations of the possible types of electronic configuration in a π system. Shown, left to right, are the positions with respect to the nonbonding level ($\epsilon = \alpha, \lambda = 0$) of the eigenvalues at positions $n/2$ and $n/2 + 1$ in open, properly closed, pseudoclosed, and meta-closed shells. In the properly closed shell, eigenvalue $n/2 + 1$ may be either antibonding as shown or strictly nonbonding.

orbital on that center to the delocalized MO. The eigenvalue λ corresponding to \mathbf{x} gives the energy ϵ of the π MO through $\epsilon = \alpha + \lambda\beta$ where α is the Coulomb integral (measuring the energy of a π electron in a p orbital on an isolated C center) and β is the resonance integral (measuring the strength of π interaction between two σ -bonded neighboring C centers). Both α and β are negative (binding) energies, and so λ can be taken as a dimensionless indicator of the MO energy, with positive λ denoting bonding.

If the eigenvalues of \mathbf{A} are arranged in nonincreasing order, two of particular interest are those of the HOMO (highest occupied molecular orbital) and LUMO (lowest unoccupied molecular orbital), which for an uncharged system with n centers (where n is even) and hence with n π -electrons, are those occurring at positions $n/2$ and $n/2 + 1$ in the order of eigenvalues, respectively. Their importance lies in the significance of a nonzero HOMO–LUMO gap as an indicator of kinetic stability and of the sum of eigenvalues up to and including the HOMO as an indicator of total π -energy and hence thermodynamic stability.

Positive eigenvalues correspond to bonding and negative eigenvalues to antibonding orbitals, and each orbital has a maximum capacity of two electrons. Electrons are assigned to orbitals in decreasing order of bonding energy (the Aufbau Principle), up to two electrons per orbital (the Pauli Exclusion Principle), adding the second electron to any one orbital only after all others at that energy have received at least one electron (Hund's Rule of Maximum Multiplicity). Fullerene π configurations are classified as follows (see Figure 2).² If the eigenvalues $\lambda_{n/2}$ and $\lambda_{n/2+1}$ are equal, then the configuration is *open-shell* (case (i)). If, conversely, $\lambda_{n/2}$ is strictly greater than $\lambda_{n/2+1}$, then three possibilities arise. If \mathbf{A} has exactly $n/2$ positive eigenvalues, $\lambda_{n/2} > 0, \lambda_{n/2+1} \leq 0$, then the neutral carbon framework has a *properly closed-shell configuration* in which all $n/2$ bonding orbitals are doubly occupied (case (ii)). If $\lambda_{n/2} > \lambda_{n/2+1} > 0$, then the neutral carbon framework has a *pseudoclosed* shell where all electrons are in doubly occupied orbitals, but some bonding orbitals are still empty (case (iii)). The final possibility, $0 \geq \lambda_{n/2} > \lambda_{n/2+1}$, is the *meta-closed* shell, where all electrons are in doubly occupied orbitals of which some are nonbonding or even antibonding (case (iv)). Meta-closed shells have not so far been encountered for neutral fullerenes, although open shells with partial occupation of formally antibonding orbitals are predicted for some large tetrahedrally symmetric fullerene graphs.¹³

2.3. Singular Graphs. A graph G is a *core graph* if G is a singular graph of nullity at least one, having a kernel eigenvector with each entry being nonzero.

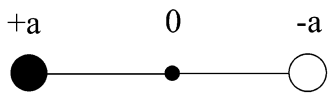


Figure 3. The path on three vertices is the smallest connected singular graph. Entries in the unique nonbonding eigenvector are shown next to the corresponding vertex, and core vertices are denoted by circles, the single periphery vertex by a dot. In this case, $F_2 = 2K_1$.

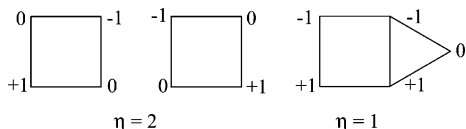


Figure 4. The cycle C_4 is a core of nullity 2 (with the two independent kernel vectors as shown). The minimal configuration is obtained by adding a single vertex to yield a graph of nullity 1, retaining the nonzero entries of the core in the kernel eigenvector.

Let \mathbf{x}_0 be a kernel eigenvector of a singular graph G of order $n \geq 3$. A subgraph of G induced by the vertices corresponding to the nonzero entries of \mathbf{x}_0 is a core $F_{\mathbf{x}_0}$ with respect to \mathbf{x}_0 . In the literature, the core is sometimes called the ‘support’ of the kernel eigenvector and can also be denoted by F_p , where p is the number of vertices of the core, called the core order.

A singular graph G of order $n \geq 3$, having core F_p and periphery $\mathcal{P} := \mathcal{V}(G) - \mathcal{V}(F_p)$, is said to be a minimal configuration, of core order p , if the following three conditions are all satisfied: (i) G is singular, with nullity one: $\eta(G) = 1$, (ii) the periphery is either empty or is a set of pairwise nonadjacent vertices: $|\mathcal{P}| = 0$ (no vertices) or \mathcal{P} induces a graph with no edges, and (iii) $\eta(F_p) = 1 + |\mathcal{P}|$.

This three-stage definition is motivated by the wish to construct extensions of a core graph that will progressively reduce the nullity and will ultimately result in a connected graph of nullity one.

Vertices that carry a zero entry in all kernel eigenvectors are said to be core-forbidden, i.e., there is no core of G that contains any of these vertices. If $\eta = 1$ the core-forbidden vertices are simply those of the periphery. In chemical terms, core-forbidden vertices are those C centers that do not acquire extra charge from occupation of the complete set of nonbonding orbitals. Figure 3 shows the smallest singular connected graph, the path on three vertices, which in chemical terms is a model for the allyl radical, and illustrates the core and periphery for this simple case. Figure 4 shows an example of how a core (in this case, the cycle on four vertices) may be extended to a minimal configuration by adding a vertex of \mathcal{P} .

It may be possible to extend a given core F_p to one or more distinct minimal configurations by drawing edges to vertices of the core from a periphery consisting of independent vertices.⁶ It is an open question whether extension to a minimal configuration of any given core can always be made.

Some remarks following from the definitions are as follows:⁶ (a) A minimal configuration is always connected and can be considered to be a graph of nullity one with a minimal number of edges and vertices for \mathbf{x}_0 .¹⁴ (b) The core of a graph of nullity one is unique, although there may be more than one distinct, and even nonisomorphic, minimal configuration which is a subgraph (see Figure 5). (c) A minimal configuration is ‘grown’ from the core F_p by adding

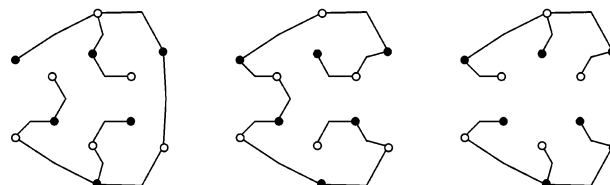
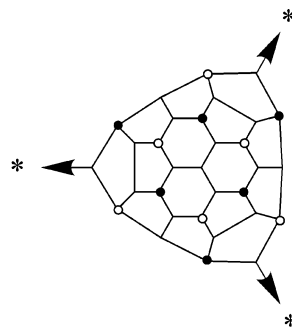


Figure 5. The singular fullerene $C_{32:5}$ has $\eta = 1$. The core vertices are independent (spanning $12K_1$) and are denoted by filled and empty circles to show the opposite signs of entries in the zero-eigenvalue eigenvector. The remaining 20 vertices form the periphery and occur as two $K_{1,3}$ ‘stars’ of four vertices plus six P_2 pairs. In this projection, chosen to exhibit the threefold symmetry of the fullerene, one vertex, marked with an asterisk, lies at infinity. Three possible minimal configurations are shown, including (center) P_{23} , the path of 23 vertices.

$\eta(F_p) - 1$ pairwise nonadjacent vertices. (d) The condition (iii) from above requires that the nullity of a minimal configuration decreases by one with each addition to F_p of a vertex of \mathcal{P} .¹⁵ (e) For minimum configurations, the core order is a maximum when $\eta(F_p) = 1$ and $n(G) = p$, when G is said to be a nut graph. It is a minimum when $\eta(F_p) = p$, and the core is the edgeless graph, i.e., $F_p = \overline{K_p}$. (f) If α is the independence number of G , then K_α is an induced subgraph of G . By interlacing, if the nullity of G is η , then $p_+ + \eta \geq \alpha$ and $p_- + \eta \geq \alpha$, p_\pm being the number of positive (negative) eigenvalues of G , counted including all repetitions (see page 19 of ref 16).

2.4. Nut Graphs. The central concept of interest in the present paper is that of the nut graph. A singular graph G is said to be a nut graph if each entry of every kernel eigenvector of G is nonzero.

A nut graph is a minimal configuration with $\mathcal{P} = 0$ and, as the name is intended to suggest, is equal to its core, so that the core order is maximum ($= n(G)$). The definition implies that $\eta = 1$ for a nut graph. (Proof: if η of some nut graph G were greater than 1, then we could take two linearly independent kernel eigenvectors of G , $\mathbf{v}_0 = (\alpha_1, \alpha_2, \dots)^T$ and $\mathbf{v}_1 = (\beta_1, \beta_2, \dots)^T$ and form $\beta_1 \mathbf{v}_0 - \alpha_1 \mathbf{v}_1 \neq 0$: this would be a kernel eigenvector with first entry zero, a contradiction.) Figure 6 shows the three smallest nut graphs, all on 7 vertices, with 8, 11, and 12 edges, respectively.

The term ‘nut graph’ is also used in journalism to signify the paragraph containing the essentials of an article; our use of the term here conveys a similar idea in that the whole of the graph is essential in the description of the null eigenvector.

Fullerenes are nonbipartite graphs (they contain odd cycles). We remark that no bipartite cubic polyhedron can be a nut graph, as the pairing of eigenvalues implies that η

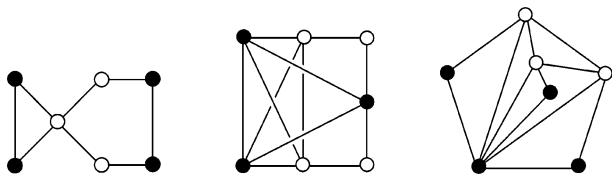


Figure 6. The three connected nut graphs are of smallest order, all on 7 vertices. Filled and empty circles denote positive and negative entries (in these cases ± 1 , respectively) in the unique zero-eigenvalue adjacency eigenvector in each case.

is even. A bipartite cubic polyhedron can, however, be a core.

3. RESULTS

3.1. Singular Fullerenes. It has already been observed in the chemical literature that singular fullerenes are mathematically possible, and indeed the second most abundant fullerene produced in experiment, C_{70} , is singular. Spiral data for singular fullerene graphs with $n \leq 60$ vertices (general fullerenes) and $n \leq 100$ vertices (isolated-pentagon fullerenes) are listed in Table 1 of ref 4. Chemical rationalizations for the occurrence of an NBO in some series of fullerenes have been presented.^{17,4} Here we will connect these considerations to the language of cores and minimal configurations.

The results of our survey of the statistics of occurrence of singular fullerenes in the range are given in Tables 1–3, which list all the singular fullerenes identified by the diagonalization calculations. The calculations employed Jacobi's method.¹⁸ Although more efficient algorithms exist, this method has the advantages of simplicity, robustness in the presence of multiplicity, and high (and tunable) numerical accuracy. Based on numerical experiments, our estimate of the precision of the eigenvalues obtained for fullerenes in our range is that it is better than 10^{-12} , i.e., several orders of magnitude smaller than is needed to distinguish reliably between small nonzero and true zero eigenvalues in graphs of this size. (In the range of n that we consider, the smallest 'small' nonzero eigenvalues have magnitudes of 10^{-5} or more.)

Table 1 gives the singular adjacent-pentagon fullerenes C_n ($20 \leq n \leq 120$), other than nut fullerenes, listed by nullity and identified by spiral number. The number of strictly positive eigenvalues is given, from which the position in the spectrum of the η null eigenvalues follows, and for $\eta = 1$ the order of the core is listed. In many cases (those marked with an asterisk in Table 1), the core consists entirely of disjoint vertices. Many of the singular fullerenes with $\eta > 1$ are themselves cores. Table 2 gives similar information for isolated-pentagon fullerenes C_n ($60 \leq n \leq 150$).

In many of the singular fullerenes of Table 1, the core consists of pairwise nonadjacent vertices, i.e., it is an independent set. These cases are marked with an asterisk in the table, and, of course, the core-order is then strictly less than $n/2$, as the fullerenes are nonbipartite polyhedra with independence numbers at most $n/2 - 2$ (achieved only if all 12 pentagons contain 2 and all $n/2 - 10$ hexagons contain 3 independent vertices: counting vertices face-by-face we have $[12 \times 2 + (n/2 - 10) \times 3]/3 = n/2 - 2$). In fact, it appears from the table that in the range of fullerenes studied, whenever the core-order is below $n/2$, the core is an independent set. It also appears from Tables 1 and 2 that

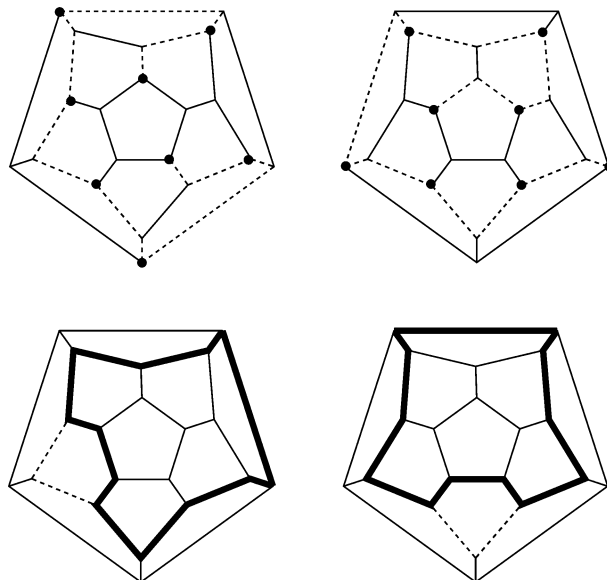


Figure 7. The smallest singular fullerene $C_{20}:1$. A set of cores for the four zero-eigenvalue eigenvectors are shown: two independent sets of order 8 (shown as filled circles) and two cycles of order 12 (shown by bold edges of the dodecahedral graph). The extra edges in the minimal configurations grown from these four cores are indicated on the diagrams by dotted lines.

the core-order of a singular fullerene with $\eta = 1$ is always even. However, in general, the core-order can be odd for trivalent polyhedra.

The smallest possible fullerene, C_{20} , is singular, with nullity 4. Its graph is that of the regular pentagonal dodecahedron, and the four NBO can be given a particularly symmetrical 'equidistributive' form by representing them as vectors of quaternions.¹⁹ The dodecahedral graph is a core, since every vertex carries a nonzero entry in some kernel eigenvector. As the nullity of the graph is 4, we can find four minimal configurations as subgraphs (not necessarily induced), by the following method: find a set of four linearly independent kernel eigenvectors of the adjacency matrix \mathbf{A} , take them as the rows of a 4×20 matrix \mathbf{B} , and apply Gaussian elimination to reduce \mathbf{B} first to row-echelon form and then to a matrix \mathbf{C} by row operations only, so that \mathbf{C} has as many zero entries as possible. The rows of \mathbf{C} are the vectors of a minimal basis of \mathbf{A} ; the nonzero entries in each row define a distinct core, and each core can be grown into a minimal configuration.⁷ The four minimal configurations obtained in this way have core orders 8, 8, 12, and 12. One choice of the four cores is illustrated in Figure 7, together with their extensions to minimal configurations of orders 15, 15, 13, and 13: thus, two of the minimal configurations are P_{15} with core $\overline{K_8}$, and the others are copies of a bicyclic graph comprising a cycle C_{12} and an additional independent vertex joined to two vertices of the core C_{12} .

The chemically realizable fullerenes confirmed to date satisfy the isolated-pentagon rule (IPR): no two pentagonal faces share a common edge. The smallest IPR fullerene is $C_{60}:1$, with the graph of the truncated icosahedron, which has no NBO. However, by introducing a cyclic chain of hexagons between the two caps of C_{60} , the graph of the smallest singular IPR fullerene, C_{70} , is obtained. This D_{5h} -symmetric fullerene has one NBO, characterized by a core that is the union of two disjoint cycles $2C_{20}$. Each C_{20} cycle

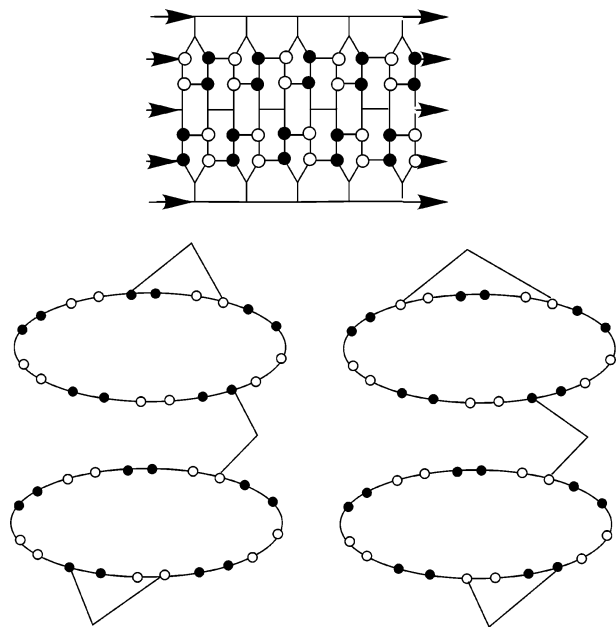


Figure 8. The smallest singular IPR fullerene, $C_{70}:1$, showing the unique zero-eigenvalue eigenvector and two noncospectral choices of minimal configuration (with core $2C_{20}$).

has $\eta = 2$, and to grow the core of $2C_{20}$ into a minimal configuration, three vertices must be added in such a way that the total nullity decreases by one at each vertex addition: the minimal configuration is thus of order 43. As $n(C_{70}:1) = 70 > 43$, there is some freedom in the choice of minimal configurations. As remarked earlier, the subgraphs that serve as minimal configurations are not necessarily isomorphic. In the present case, they are not even cospectral (see Figure 8).

The construction can be continued indefinitely.¹⁷ An infinite family of tubular fullerenes, C_n , with hemi- C_{60} caps and nullity one, has members at $n = 70 + 30m$, ($m = 0, 1, 2, \dots$) with overall 5-fold symmetry. The core of each consists of the disjoint union of $m + 2$ copies of C_{20} cycles. In each case, a minimal configuration is a subgraph of the fullerene with $20(m + 2) + [2(m + 2) - 1] = 22m + 43$ vertices. The fullerenes $C_{70}:1$, $C_{100}:1$, and $C_{130}:1$ in Table 2 belong to this class and, as the entries in the table confirm, have the 35, 50, and 65 strictly positive eigenvalues needed for a properly closed shell and the 40, 60, and 80 nonzero entries in their zero-eigenvalue eigenvectors consistent with the description of the core as multiple disjoint copies of C_{20} .

A second family has members at $n = 84 + 36m$, ($m = 0, 1, 2, \dots$), with hemi- C_{72} caps, overall 6-fold symmetry and nullity one for $m > 0$. For $m > 0$, the core consists of the disjoint union of $m + 2$ copies of C_{24} , and a minimal configuration is a subgraph of the fullerene with $24(m + 2) + [2(m + 2) - 1] = 24m + 51$ vertices. Table 2 includes the member of the series with $m = 1$, $C_{120}:10$ 606. The $m = 0$ member of the series fullerene $C_{84}:1$ has an accidental degeneracy of the zero eigenvalue and has nullity 3. A minimal basis for the nullspace has three linearly independent kernel eigenvectors, each of which corresponds to a core that can be extended to a subgraph which is a minimal configuration. One of the cores of $C_{84}:1$, for the eigenvector generic to the $n = 84 + 36m$ series, is $2C_{24}$, but as $\eta > 1$, the graph of $C_{84}:1$ has other cores in addition. Only the 12

equatorial vertices of $C_{84}:1$ carry zero entries in all cores, i.e., are core-forbidden.

The generic nondegenerate NBO in the two series of 'carbon cylinders' has been rationalized in terms of nodal patterns for cylindrical harmonics.¹⁷ Each was shown to have nonzero entries on disjoint C_{20} or C_{24} subgraphs of the fullerene cylinder, each cycle carrying entries with paired signs $\dots ++ -- ++ \dots$, the cycles being separated from one another by belts of vertices carrying zero entries in the null eigenvector. The polygons at the 'poles' of the cylinder (pentagons for the series $70 + 30k$, hexagons for $84 + 36k$) and their direct neighbors also carry zero entries. This description based on chemical/physical analogy has an exact counterpart in the core/minimal configuration picture, as we have seen.

3.2. Nut Fullerenes. An interesting aspect of the fullerene class, apparently unremarked before these studies began,^{8,9} is that it includes nut graphs. Thus, we can answer in the affirmative the first question posed in the Introduction.

Table 3 lists data on the 41 nut graphs found among the 10 190 782 fullerenes in the range $20 \leq n \leq 120$. All have pentagon adjacencies. Isolated-pentagon fullerenes, which include all those that have been physically characterized, were checked up to $n \leq 150$, and no nut graph or core of nullity more than one was found among them. For each adjacent-pentagon nut fullerene, a lexicographically minimal spiral is listed, together with the point group symmetry of the fullerene, symmetry of the unique null eigenvector, number of positive eigenvalues, and a characterization (to be discussed below) of the type of eigenvector as 'uniform', 'balanced', or 'other'.

Spectrum. The nut-fullerenes show a pattern in the number of positive eigenvalues p_+ ; in all but two of the listed nut fullerenes (42:12 and 60:1279), p_+ is equal to $n/2 + 2$, which is also the number of faces in the fullerene. The fact that $p_+ > n/2$ is compatible with the observation of electron deficiency in fullerene molecules: most fullerenes (singular or not) have pseudoclosed π shells and therefore have a capacity for accepting electrons over and above the neutral electron count. The NBO is at position $n/2 + 2$ or $n/2 + 3$ for all the nut fullerenes found so far. Thus the NBO would typically be the HOMO of C_n^{4-} or C_n^{6-} . Alternatively, it would be the LUMO of C_n^{2-} or C_n^{4-} . In particular, p_+ is equal to $n/2 + 2$ for all the nut fullerenes labeled 'uniform' in the table. In other words, the number of strictly positive eigenvalues exceeds the number of strictly negative eigenvalues by 5 in these cases. In the neutral molecule, the uniform nut fullerenes of Table 3 all have pseudoclosed shell electronic configurations with two empty bonding orbitals below a nonbonding LUMO+2.

Symmetry. All but one of the nut-graph fullerenes found in the search have a C_2 symmetry element (42:12 is the exception), and, in fact, most have D_2 symmetry, signaling the presence of three mutually perpendicular C_2 axes. The D_{2h} and D_{2d} supergroups of D_2 , where the symmetries are augmented by three orthogonal mirror planes, or by two orthogonal mirror planes and a fourfold axis of improper rotation, respectively, also appear in the list of nut-fullerene point groups. Figure 9 shows the three-dimensional structures of the first 24 nut fullerenes, drawn from their topological coordinates.²⁰

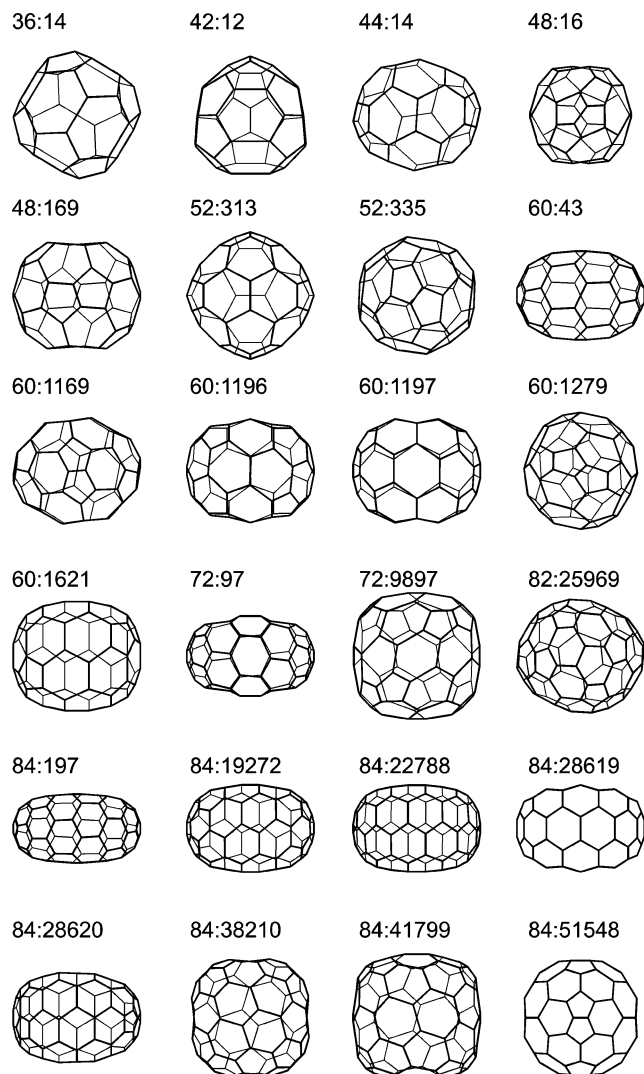


Figure 9. Structures of the first 24 nut fullerenes. Fullerenes are listed by vertex count and position in the general spiral order. Symmetry and spectral properties are listed in Table 3.

The irreducible representations of the NBO eigenvector are listed in Table 3 (column ‘ Γ ’). It is notable that within their respective point groups, all but two of the nut fullerenes found in the search have totally symmetric NBO eigenvectors (i.e., with representation a_1 in D_{2d} , a_g in D_{2h} , a in D_2 , and C_2 , a' in C_s).²¹ Every operation of the point group permutes vertices that carry equal coefficients in such a vector. The totally symmetric nature of the NBO in a wide class of nut trivalent polyhedra can be proved, as will be seen below.

3.2.1. Balanced and Uniform Nut Fullerenes. Further insight into the structure of the null eigenvectors in nut graphs can be gained by looking at the possible patterns of entries and signs in such vectors. The construction of nonbonding orbitals in π -systems has a long history in chemistry.^{22,23} The eigenvalue condition $\mathbf{Ax} = \lambda\mathbf{x}$ for eigenvalue λ implies that the entries for any zero-eigenvalue eigenvector, $\mathbf{x} = \{x_i\}$, of the (trivalent) graph G should obey $\sum x_j = 0$ for all i ($i = 1, \dots, n$), where the summation runs over all (three) neighbors j of a vertex i . The nullity of a given graph may therefore be established by a simple construction, without the need to obtain the full spectrum: begin with any vertex, assign parameters for the entries on all but one of its neighbors, define the entry for the last neighbor as the negative of the

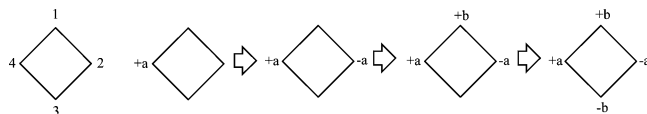


Figure 10. Pencil-and-paper approach to determining nullity, illustrated for the 4-cycle, C_4 . Assign a , $-a$ to the neighbors of 1 and then assign b , $-b$ to the neighbors of 2. Now all vertices carry a value. Check that 3 and 4 obey the zero-sum rule. As they do, there are two independent parameters, so the nullity of the 4-cycle is $\eta = 2$, in agreement with the well-known result for the antiaromatic $4n$ -cycles.

sum of the others, then choose another (nearby) vertex, make the assignment of its unassigned neighbors, and in this way work around the graph, assigning new parameters as necessary, until all vertices carry a value, and then finally eliminate redundant parameters by invoking the zero sum rule at every vertex that has not so far been used. The number of independent parameters remaining after this elimination is $\eta(G)$, the nullity of the graph. A simple example of the construction is shown in Figure 10.

This reasoning also provides the basis for a classification of kernel eigenvectors in trivalent polyhedra such as fullerenes. Assign labels a , b , and c to the three entries on the neighbors of a typical vertex. Three independent, normalized combinations of three quantities are one totally symmetric combination

$$S_0 = \frac{1}{\sqrt{3}}(a + b + c)$$

and a pair that are symmetric/antisymmetric with respect to an imagined mirror plane containing both the vertex with entry a and the central vertex and passing between b and c :

$$S_{1s} = \frac{1}{\sqrt{6}}(2a - b - c)$$

$$S_{1a} = \frac{1}{\sqrt{2}}(b - c)$$

S_0 vanishes at every vertex, by definition of a null vector. Thus, around any vertex of a trivalent nut graph, the pattern (a, b, c) can be characterized by the local values of S_{1s} and S_{1a}

$$a = \sqrt{\frac{2}{3}}S_{1s}, \quad b = \sqrt{\frac{1}{6}}S_{1s} + \sqrt{\frac{1}{2}}S_{1a},$$

$$c = -\sqrt{\frac{1}{6}}S_{1s} - \sqrt{\frac{1}{2}}S_{1a}$$

with the constraint that S_{1s} may not be zero, since a cannot vanish in a nut graph, though S_{1a} may take value zero or any value other than $\pm\sqrt{(1/3)}S_{1s}$.

Consider the case where S_{1a} can be made zero for every vertex, by appropriate ordering of a , b , and c , i.e., in the unique null eigenvector every vertex has equal entries $b = c$ on two of its neighbors, cancelled by an entry $a = -2b$ on the third. The numerical value of a may be different for different central vertices. We call a trivalent nut graph with this property a *nut-balanced* or simply a *balanced* graph.

If furthermore, every vertex has the *same* triple of neighboring entries (up to ordering), then a balanced graph is called *nut-uniform* or simply *uniform*. In a uniform nut

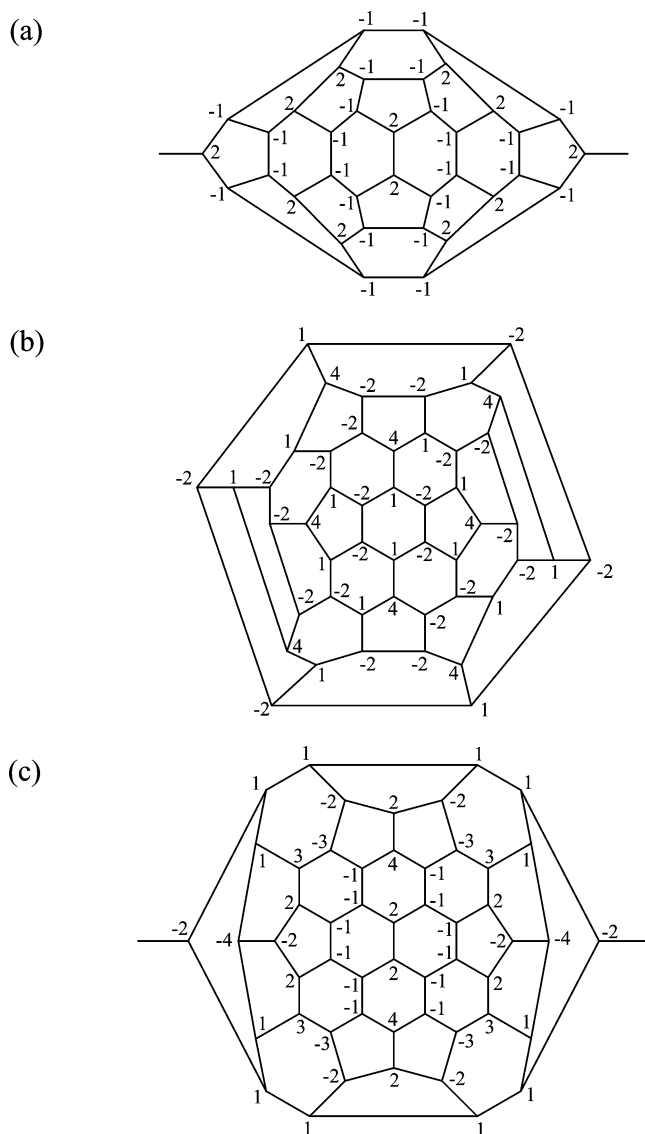


Figure 11. Patterns of coefficients in the null eigenvectors of the smallest nut fullerenes of each type: (a) the smallest uniform nut fullerene 36:14; (b) the smallest balanced but not uniform nut fullerene 48:169; and (c) a nut fullerene that is neither uniform nor balanced 52:313.

graph, every vertex has the same neighboring entries in the ratio 1:1:−2 in the unique zero-eigenvalue eigenvector, with $2n/3$ vertices bearing coefficient $1/\sqrt{2n}$ and $n/3$ bearing $-2/\sqrt{2n}$ in the normalized vector.

Figure 11 shows the pattern of coefficients in the null eigenvectors for small examples of uniform, balanced and general nut fullerenes. In the range to $n = 120$, there is only one fullerene that is balanced but not uniform (48:169).

The chemical significance of the definition of the uniform nut fullerene is that these have the smallest ratio between magnitudes of smallest and largest entries in the null eigenvector and thus would have the ‘smoothest’ distribution of spin density in a radical where the NBO was the singly occupied HOMO.

3.2.2. Eigenvector Entries of Balanced Cubic Nut Graphs. Consideration of the way that the zero-sum condition propagates through a trivalent graph shows that balanced trivalent nut graphs are the generalization of uniform nut graphs in which the kernel eigenvector has entries (apart from

normalization) in the set $\{1, -2, 4, -8, \dots, (-2)^r, \dots\}$, for integer r . If k is the largest integer r that appears in the coefficients $(-2)^r$ of \mathbf{x} , then *all* the integers from 0 to k appear in the coefficients; i.e. the entries of \mathbf{x} are $1, -2, 4, \dots, (-2)^k$, possibly with repetitions. A proof of this statement is as follows: If there exists $j, 0 \leq j \leq k$, such that $(-2)^j$ is missing from the coefficients of \mathbf{x} , then for a suitable labeling of G

$$\mathbf{x} = (1, \dots, 1, -2, \dots, -2, \dots, (-2)^{j-1}, \dots, (-2)^{j-1}, (-2)^{j+i}, \dots, (-2)^{j+i}, \dots, (-2)^k, \dots, (-2)^k)$$

where $i > 0$. Thus, two linearly independent kernel eigenvectors can be found, namely

$$\mathbf{x}_1 = (1, \dots, 1, -2, \dots, -2, \dots, (-2)^{j-1}, \dots, (-2)^{j-1}, 0, \dots, 0)$$

and

$$\mathbf{x}_2 = (0, \dots, 0, (-2)^{j+i}, \dots, (-2)^{j+i}, \dots, (-2)^k, \dots, (-2)^k)$$

and G is not a nut. Therefore the sequence of powers of -2 cannot have a gap.

Various relations hold between the numbers of entries for different powers of two. Let $n_1, n_{-2}, \dots, n_{(-2)^k}$ denote, respectively, the number of coefficients $1, -2, \dots, (-2)^k$ that appear in \mathbf{x} . Then

$$n_1 - 2n_{-2} + 4n_4 - \dots + (-2)^k n_{(-2)^k} = 0 \quad (\star)$$

This result follows by straightforward counting: let h_1 denote the number of vertices with first neighbors having \mathbf{x} -coefficients $1, 1, -2$, and let h_{-2} the number with first neighbors having \mathbf{x} -coefficients $-2, -2, 4$, and so on. Then

$$n_1 = 2h_1$$

$$n_{-2} = h_1 + 2h_{-2}$$

$$n_4 = h_{-2} + 2h_4$$

⋮

$$n_{(-2)^{k-1}} = h_{(-2)^{k-2}} + 2h_{(-2)^{k-1}}$$

$$n_{(-2)^k} = h_{(-2)^{k-1}}$$

Multiplying the r th equation by $(-2)^r$ for $0 \leq r \leq k$ and adding all the equations, the sum rule (\star) follows.

3.2.3. Allowed Orders of Balanced Cubic Nut Graphs.

The same reasoning can be used to show that the vertex count of any balanced cubic nut graph is a multiple of six. The proof is an immediate consequence of the preceding: given that when the vertices of each type are all counted we recover n , the total number of vertices in G , we have

$$n_1 + n_{-2} + n_4 + \dots + n_{(-2)^k} = n$$

and summation of the individual expressions listed above gives

$$n = 3(h_1 + h_{-2} + h_4 + \dots + h_{(-2)^{k-1}})$$

and as n for a 3-regular graph is even, the vertex count of a balanced trivalent nut polyhedron is divisible by 6. Specif-

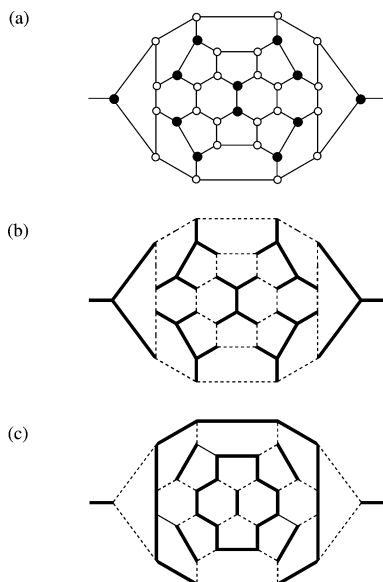


Figure 12. The null eigenvector of a balanced (and uniform) nut fullerene, $C_{36}:14$. Illustrations of (a) the null eigenvector pattern of -2 (black-filled circles) and $+1$ (white-filled circles); (b) the spanning of a nut fullerene graph C_n by $n/6$ disjoint motifs consisting of a $(-2, -2)$ edge with its four neighboring $(-2, +1)$ edges; and (c) the subgraph induced by the -2 and the $+1$ entries of the null eigenvector; the first graph is a union of pairs, and the second is a union of cycles.

ically, therefore, all balanced nut fullerenes (and hence also uniform nut fullerenes) have vertex counts $24 + 6q$ for some q .

In a uniform trivalent polyhedron the entries occur as $n/6$ disjoint pairs $(-2, -2)$, $2n/3$ pairs $(-2, +1)$, and $2n/3$ pairs $(+1, +1)$. The graph of the uniform nut fullerene is therefore spanned by $n/6$ disjoint motifs consisting of a $(-2, -2)$ -edge with its four neighboring $(-2, +1)$ -edges. The graph induced by the -2 entries is the disjoint union of K_2 pairs, and the graph induced by the $+1$ entries is a union of cycles (Proof: every $+1$ has two $+1$ neighbors, and every -2 has one -2 neighbor.) Figure 12 shows these graphs for the smallest nut fullerene, $C_{36}:14$.

3.2.4. Symmetry of the Zero-Eigenvalue Vector. As Table 3 shows, most (32 out of 41) of the nut fullerenes found in the range are balanced, and in fact all but one of the balanced nut fullerenes are uniform. The table also shows that all the balanced nut fullerenes have a totally symmetric null eigenvector, i.e., a vector that transforms into itself under all operations of the point group. Just two instances of nontotally symmetric zero eigenvectors are seen in the table (52:313 and 52:335).

From the special form of the entries in the unique kernel eigenvector of a balanced nut trivalent polyhedron, it is straightforward to show that this vector *must* be totally symmetric. Additionally, an eigenvector \mathbf{x} of \mathbf{A} is said to be *equidistributive* if the entries of \mathbf{x} have the same absolute value on equivalent vertices (i.e., vertices in the same orbit).¹⁹ A vector composed of the squared entries of an equidistributive vector would be totally symmetric; all nondegenerate eigenvectors are therefore equidistributive, and in particular, as the unique kernel eigenvector of a nut graph is of multiplicity one, it must be equidistributive. For balanced nut graphs, this vector is not only equidistributive but totally symmetric.

For nut graphs that are neither uniform nor balanced, the kernel eigenvector may have one of several nondegenerate symmetries, and the entries in \mathbf{x} may take general integer values (as for any eigenvector corresponding to an integer eigenvalue).

3.2.5. Nut Fullerenes and Pentagon Adjacency. One striking feature of the nut fullerenes found within the scope of the search is that all of them have some pentagon–pentagon adjacencies. The numbers of pentagon–pentagon edges (N_p) listed in Table 3 range from 2 to 14.

It is straightforward to show that any *uniform* nut fullerene must have some pentagon adjacencies, and more precisely that every pentagon of a uniform nut fullerene must be adjacent to at least one other, so that the number of adjacencies is $N_p \geq 6$ for such fullerenes. The proof is pictorial. A fullerene in which at least one pentagon is fully isolated from all others contains the ‘corannulene’ structural motif shown in Figure 13. If the fullerene is a uniform nut graph, then this motif can be decorated consistently with the $\{-2, +1\}$ entries of the unique null eigenvector. The central pentagon may carry zero, one, or two entries equal to -2 , and if two such entries are present, then they must be on adjacent vertices; all other cases are ruled out by the requirement that no vertex has two -2 neighbors. As Figure 13 shows, all three distributions on the central pentagon lead to a contradiction of the assumed uniformity of the nut fullerene. Thus, no uniform nut fullerene may contain a fully isolated pentagon. Therefore, all uniform nut fullerenes contain at least six pentagon–pentagon edges.

3.2.6. Infinite Families of Singular Fullerenes. Inspection of the pictures (Figure 9) and spiral codes (Table 3) of the early nut fullerenes suggests some recurring patterns.

As the vertex count increases, cylindrical nut fullerenes occur and can be grouped into families according to their six-pentagon caps. Thus, for example, uniform nut fullerenes with the spiral

$$1, 2, 3, 4, 7, 10, n/2 - 6 - \delta, n/2 - 3 - \delta, \\ n/2 - 1, n/2, n/2 + 1, n/2 + 2$$

where the parameter δ cycles through 0, 1, 1 can be seen in Table 3 at 48:16, 60:43, 72:97, 84:197, 96:367, 108:634, and 120:1069. This is a family of tubular fullerenes, each with a cap of six pentagons and two hexagons, circumscribed by successive rings of six hexagons and ending with the same cap. As Figure 14 shows, a kernel eigenvector with entries $\{-2, +1, +1\}$ can be propagated uniformly, with the same cyclic sequence on all intermediate perimeters, to terminate smoothly on the other cap. The pattern of coefficients is compatible with insertion of any number of extra layers of six hexagons in the starting C_{48} structure, so that we have an infinite series of singular fullerenes, with predictable spiral codes. All members of the series are cores. Although we have no formal proof that the multiplicity of the zero eigenvalue remains at one after each stage of the expansion, the null eigenvector in each member of the series is found to remain unique at least for all $n \leq 1000$, and it appears plausible that we have an infinite family of not only core fullerenes but also uniform-nut fullerenes.

Other series can also be found, some with multiple isomers arising from relative rotation of the end caps and with more complicated sequences of perimeters. Two examples are

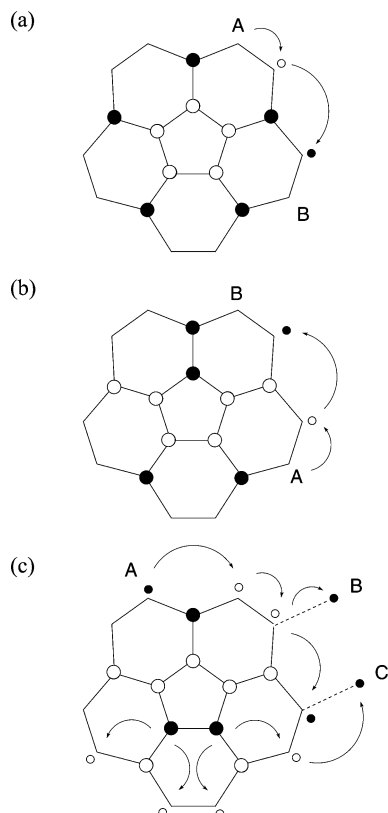


Figure 13. Pictorial proof that no uniform nut fullerene can have a fully isolated pentagonal face. White-filled circles stand for +1 entries in the null eigenvector, black-filled circles stand for -2 entries. The five entries on the pentagon determine, among others, the entries on radiating edges, shown as large circles. (a) The central pentagon carries no entry -2. Begin assigning the remaining vertices at A: its -2 neighbor implies a neighbor +1, which implies a -2 as indicated by the arrows; B then has two -2 neighbors, in contradiction of the uniform nut property. (b) The central pentagon carries a single entry -2. Begin assigning the remaining vertices at A: its -2 neighbor implies a +1, then a -2, therefore giving B two -2 neighbors, in contradiction of the uniform nut property. (c) The central pentagon carries two entries -2. The -2 entries on the pentagon determine, among others, the (small circle) +1 entries on their second neighbors. The entry at A may be chosen without loss of generality as -2, leading to -2 at B and C. As every ring of the fullerene is either a pentagon or a hexagon, *either* B is joined to C by an edge, in which case C has two -2 neighbors, *or* B is joined to C through an intermediate vertex that itself has two -2 neighbors, in both cases contradicting the uniform nut property.

shown in Figure 15. Expansion of the cap shown in Figure 15(a) is particularly straightforward, with face spirals generated by adding multiples of 24 hexagons between the sixth and seventh pentagons in the face spirals of the parent cages 60:1196, 60:1197, and 84:19272 (see Table 3). Again all members of the series with $n \leq 1000$ have been checked to be uniform nut fullerenes. It is an open question whether such tubular extensions can be found for *every* uniform nut fullerene and whether families might also exist for the nonuniform nut fullerenes. Similar constructions may be expected for non-fullerene trivalent graphs.

4. GENERAL TRIVALENT POLYHEDRA

To give some context to the results for nut fullerenes, a survey was made of nut graphs among small general cubic polyhedra. Table 4 gives statistical data on the general cubic polyhedra on up to 24 vertices. Singular graphs are common

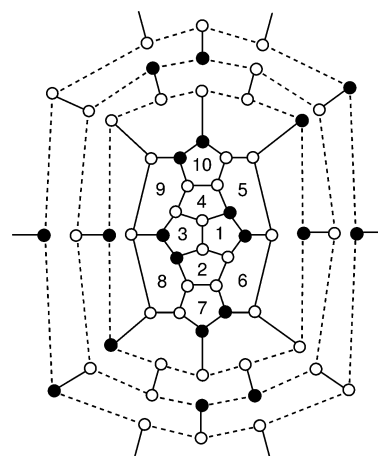


Figure 14. An expansion construction for uniform nut fullerenes. The example is the expansion of one of the two identical caps of 48:16. Working out from the central motif of six pentagons, preservation of the uniform pattern of -2 and +1 entries around each vertex (black- and white-filled circles) in the null eigenvector demands the pattern $(-2, -2, +1, +1, +1, +1)^2$ on the outer perimeter of each circuit of added six hexagons, which then repeats until closure by a similar cap.

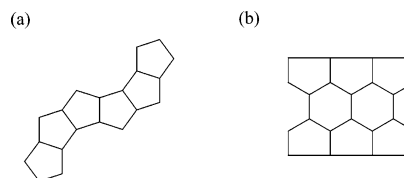


Figure 15. Caps from which an infinite series of uniform nut fullerenes can be constructed. (a) The six-pentagon snake cap of the D_{2+} series 36:14, 60:1196, 60:1197, 84:19272, 108:140651, 108:140652, The cap is filled out with hexagons, then circumscribed with hexagon strips presenting perimeters of type $(-2, -2, +1, +1)_4$ and $(-2, +1, +1, +1)_4$, and can be terminated consistently with a (rotated) copy of the same cap, to give a uniform null-eigenvector. (b) A six-pentagon cap that can also be built up by circumscribing, in this case with perimeters consisting of either +1 entries only, or of $(-2, -2, +1, +1)$ units, and terminated consistently with a (rotated) copy of the same cap.

in this range: at $n = 12$, 11 of the 14 cubic polyhedra are singular, and, overall about a third (133 887) of the 398 438 cubic polyhedra on up to 24 vertices are singular, 93 197 of them with $\eta = 1$. The numbers of bipartite cubic polyhedra in this range are small, but, for example, 30 of the 32 cases with $n = 24$ are singular, with $\eta = 2$ or $\eta = 4$. Nut graphs are found at $n = 12, 18$, and 24, including almost one in five of the cubic polyhedra with these numbers of vertices. Over half are uniform, but the balanced and general nut graphs are also represented. Interestingly, no nut graphs with n not divisible by 6 are found in this range, although we know from the fullerene results (Table 3) that nonbalanced cubic polyhedral nuts with such vertex counts do exist.

Figure 16 shows the smallest examples of singular cubic polyhedra with $\eta = 1, 2, 3, 4, 5$. Figure 17 shows the two smallest nut-graph cubic polyhedra, each uniform, one with C_2 and one with the trivial C_1 symmetry, and also shows an example of a cubic polyhedron that is an unbalanced nut graph.

These results can be extended. Figure 18 illustrates a construction that can be used to generate arbitrarily large singular non-fullerene cubic polyhedra, starting from any singular cubic polyhedral graph. An adjacency eigenvector

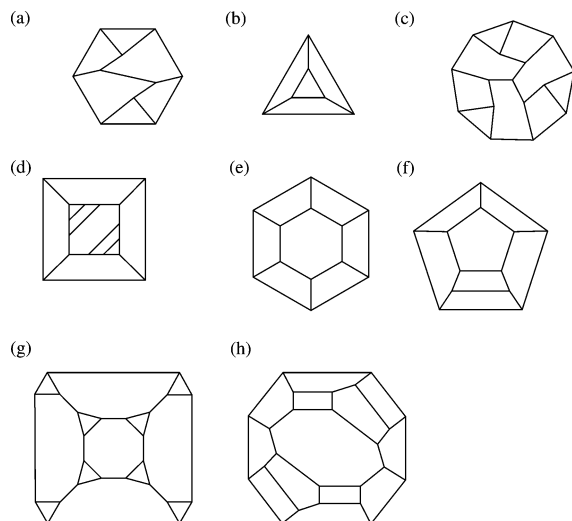


Figure 16. The smallest singular cubic polyhedra with nullity $\eta = 1-5$. The polyhedra are numbered according to their vertex count n , position in the order of generation by the plantri program¹⁰ and point symmetry group. (a) $\eta = 1$ (10:1, C_2); (b) $\eta = 2$ (6:1, D_{3h}); (c) $\eta = 3$ (16:69, C_3); (d) $\eta = 3$ (16:206, C_{2v}); (e) $\eta = 4$ (12:5, D_{6h}); (f) $\eta = 4$ (12:14, D_{2d}); (g) $\eta = 5$ (24:235 618, O_h); (h) $\eta = 5$ (24:272 254, D_2).

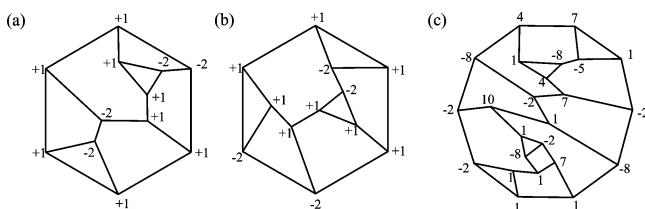


Figure 17. Small cubic polyhedral nut graphs and their null eigenvectors. The smallest cubic polyhedra with nut graphs as skeletons are (a) 12:2 (C_2) and (b) 12:6 (C_1). Both are uniform nut graphs. (c) Cubic polyhedral nut graphs that are neither uniform nor balanced occur first at 24 vertices. An example (24:64) in which the spin density would span a ratio of 100:1 is shown here.

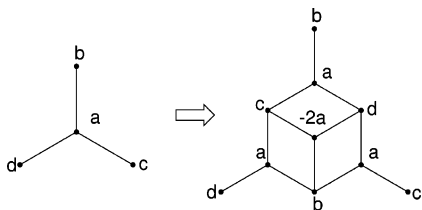


Figure 18. An expansion of cubic graphs that preserves null eigenvectors. The central vertex carries entry a and in a null eigenvector the entries on its neighbors total $b + c + d = 0$. Expansion of the central vertex to a half-cube, as shown on the right, can be achieved without disruption of the null eigenvector if new eigenvector entries are assigned as shown. Clearly, if the parent graph is a uniform nut graph and $a = +1$, then the derived vector is uniform, but if $a = -2$, then the derived vector is only balanced. Conversely, if the parent vector is only balanced, then so is the derived vector.

corresponding to a zero eigenvalue of an n -vertex trivalent graph can be converted to an eigenvector with the same eigenvalue for a $(n + 6)$ -vertex trivalent graph by an expansion that raises a half-cube on any one of the original vertices. Iteration leads to an infinite series of singular cubic graphs, each with at least the nullity of its parent. Barring accidents that introduce new possibilities for zero eigenvalues, this construction generates nut graphs from nut-graph parents. As illustrated in the figure, the expansion *always*

preserves the balanced nature and *may* preserve the uniform nature of a null eigenvector. The half-cube construction accounts at least partly for the rapid growth in the number of nut graphs in Table 3. The two original 12-vertex nut graphs generate 6 + 12 nonisomorphic 18-vertex nut graphs, and these then generate a total of 228 distinct nut graphs (103 uniform and 125 balanced) at $n = 24$. Large, and symmetrical, singular polyhedra can be constructed using the half-cube construction: expansion of the dodecahedron ($\eta = 4$) on all 20 of the original vertices, for example, gives a 140-vertex polyhedron with full I_h symmetry, 60 4-gonal and 12 15-gonal faces, and with $\eta = 4$ and $n/2 - 1$ positive eigenvalues.

5. CONCLUDING REMARKS

It has been shown that some fullerenes are nut graphs—graphs with a single null eigenvector in which all entries are nonzero. All examples found so far have multiple pentagon adjacencies, and it was proved that no uniform nut fullerene contains isolated pentagons. In the examples found so far, occupation of the single nonbonding orbital requires an excess negative charge on the fullerene. However, some fullerenes, though not qualifying as nut graphs, may be considered as in some sense near to nut graphs. For instance, there are ten singular isolated-pentagon fullerenes for $n \leq 120$, all of nullity one except C_{84} isomer 24 which has nullity three. None of them are nut graphs, though C_{106} and C_{114} , as ‘sporadic’ closed shell fullerenes,² approach ‘nut graph status’ as they each have an eigenvalue very close to but not exactly zero. Another measure of proximity to nut graphs might be the size of the core in the kernel eigenvector of a graph with $\eta = 1$. Examples of such near-nut graphs are 96:170 895, with 94 nonzero entries, and the isolated-pentagon fullerene 100:285 901 (=100:438), with 96 nonzero-entries.

From the chemical point of view, small polyhedra may seem unlikely models for carbon cages because they include small rings, with consequent angle strain, but explorations of the sets of isomeric possibilities with 20 and 24 vertices suggest that many, if not all, occupy at least local minima on the potential energy surfaces for these numbers of carbon atoms.²⁴ Interestingly, for most of the nut graphs among these polyhedra, as listed in Table 4, the null eigenvalue is at position $n/2$, i.e., it would be the doubly occupied HOMO of the π system of the neutral cage, and in the singly charged radical cation the nut nature of the graph would be predicted to lead to nonzero spin density on all atoms. This contrasts with nut fullerenes, where, as discussed in section 3.2, occupation of the NBO requires a high negative charge. The two nut graphs with $n = 12$, some 262 of the nut graphs with $n = 18$, and 54 699 of those with $n = 24$ have adjacency spectra with the requisite $(n/2 - 1)$ positive and $n/2$ negative eigenvalues.

Finally, it may be interesting to note that although chemical fullerenes have planar graphs, nut graphs are not confined to those of genus zero. Analogues of the fullerenes can be defined among nonplanar graphs:²⁵ those that can be embedded in the projective plane are constructed by collapsing antipodal vertices of centrosymmetric conventional fullerenes, relying on the fact that the sphere is a double cover of the projective plane. The eigenvectors of the projective-plane graph follow by collapse of the *gerade* eigenvectors of the

spherical fullerene, preserving the eigenvalue. As the kernel eigenvector of any balanced nut fullerene is totally symmetric, antipodal collapse of a centrosymmetric balanced nut fullerene leads to a projective-plane fullerene that is also a balanced nut graph. The centrosymmetric nut fullerenes with $n \leq 100$ are 84:28 619 (D_{2h} , uniform) and 84:51 548 (D_{2h} , neither uniform nor balanced), and both yield 42-vertex projective-plane nut fullerenes on antipodal collapse. Collapse of a centrosymmetric fullerene with $\eta > 1$ could also conceivably lead to a nut graph.

REFERENCES AND NOTES

- (1) Fowler, P. W.; Ceulemans, A. Electron deficiency of the fullerenes. *J. Phys. Chem.* **1995**, *99*, 508–510.
- (2) Fowler, P. W.; Manolopoulos, D. E. *An atlas of fullerenes*; Oxford University Press: Oxford, U.K., 1995; Dover Publications Inc.: New York, 2007.
- (3) Brinkmann, G.; Dress, A. W. M. A constructive enumeration of fullerenes. *J. Algorithms* **1997**, *23*, 345–358.
- (4) Yoshida, M.; Fujita, M.; Fowler, P. W.; Kirby, E. C. Non-bonding orbitals in graphite, carbon tubules, toroids and fullerenes. *J. Chem. Soc., Faraday Trans.* **1997**, *93*, 1037–1043.
- (5) Ceulemans, A.; Chibotaru, L. F.; Bovin, S. A.; Fowler, P. W. The electronic structure of polyhex carbon tori. *J. Chem. Phys.* **2000**, *112*, 4271–4278.
- (6) Sciriha, I. On the construction of graphs of nullity one. *Discrete Math.* **1998**, *181*, 193–211.
- (7) Sciriha, I. On the Rank of Graphs. In *The Eighth Quadrennial International Conference on Graph Theory, Combinatorics, Algorithms and Applications*; Alavi Y., Ed.; Springer-Verlag: Berlin, Germany, 1998; Vol. II, pp 769–778.
- (8) Sciriha, I.; Fowler, P. W. A spectral view of fullerenes. *Math. Balkanica* **2004**, *18*, 183–192.
- (9) Sciriha, I.; Fowler, P. W. On nut and core singular fullerenes. *Discrete Math.* In press.
- (10) Brinkmann, G.; McKay, B. D. Fast generation of planar graphs. To appear in *MATCH Commun. Math. Comput. Chem.* **2007**. See also <http://cs.anu.edu.au/bdm/plantri> (accessed Jan 1, 2007).
- (11) Grünbaum, B.; Motzkin, T. S. The number of hexagons and the simplicity of geodesics on certain polyhedra. *Can. J. Math.* **1963**, *15*, 744–751.
- (12) See, e.g., Streitwieser, A. *Molecular orbital theory for organic chemists*; Wiley: New York, 1961 or Salem, L. *The molecular orbital theory of conjugated Systems*; W. A. Benjamin Inc.: New York–Amsterdam, 1966.
- (13) Fowler, P. W. Fullerene graphs with more negative than positive eigenvalues: the exceptions that prove the rule of electron deficiency? *J. Chem. Soc., Faraday Trans.* **1997**, *93*, 1–3.
- (14) Sciriha, I.; Gutman, I. Minimal configuration trees. *Linear Multilinear Algebra* **2006**, *54* 141–145.
- (15) Sciriha, I.; Gutman, I. Minimal configurations and interlacing. *Graph Theory Notes N.Y.* **2005**, *49*, 38–40.
- (16) Cvetković, D.; Doob, M.; Sachs, H. *Spectra of graphs - Theory and application*; Johann Ambrosius Barth Verlag: Heidelberg-Leipzig, Germany, 1995.
- (17) Fowler, P. W. Carbon cylinders: A class of closed-shell clusters. *J. Chem. Soc. Faraday* **1990**, *86*, 2073–2077.
- (18) Press, W. H.; Flannery, B. P.; Teukolsky, S. A.; Vetterling, W. T. *Numerical recipes. The art of scientific computing*; Cambridge University Press: Cambridge, U.K., 1986.
- (19) Ceulemans, A.; Fowler, P. W.; Szopa, M. Quaternions and equidistributive eigenvectors of symmetric graphs. *Math. Proc. R. Irish Acad.* **1998**, *98A*, 139–151.
- (20) Manolopoulos, D. E.; Fowler, P. W. Molecular graphs, point groups and fullerenes. *J. Chem. Phys.* **1992**, *96*, 7603–7614.
- (21) Atkins, P. W.; Child, M. S.; Phillips, C. S. G. 1970 *Tables for group theory*; Clarendon Press: Oxford, U.K., 1970.
- (22) See e.g., Trinajstić, N. *Chemical graph theory*, 2nd ed.; CRC Press: Boca Raton, FL, 1992.
- (23) Longuet-Higgins, H. C. Some studies in molecular orbital theory I. Resonance structures and molecular orbitals in unsaturated hydrocarbons. *J. Chem. Phys.* **1950**, *18*, 265–274.
- (24) Domene, M. C.; Fowler, P. W.; Mitchell, D.; Seifert, G.; Zerbetto, F. Energetics of C_{20} and C_{22} fullerene and near-fullerene carbon cages. *J. Phys. Chem. A* **1997**, *101*, 8339–8344.
- (25) Deza, M.; Fowler, P. W.; Rassat, A.; Rogers, K. M. Fullerenes as tilings of surfaces. *J. Chem. Inf. Comput. Sci.* **2000**, *40*, 550–558.

CI700097J